

2011

Vacancies, twins, and the thermal stability of ultrafine-grained copper

C. Saldana

Pennsylvania State University

Alexander H. King

Iowa State University, alexking@ameslab.gov

E. A. Stach

Brookhaven National Laboratory

W. D. Compton

Purdue University

S. Chandrasekar

Purdue University

Follow this and additional works at: http://lib.dr.iastate.edu/ameslab_pubs



Part of the [Materials Science and Engineering Commons](#)

The complete bibliographic information for this item can be found at http://lib.dr.iastate.edu/ameslab_pubs/2. For information on how to cite this item, please visit <http://lib.dr.iastate.edu/howtocite.html>.

Vacancies, twins, and the thermal stability of ultrafine-grained copper

Abstract

Ultrafine-grained metals have impressive strength but lack the thermal stability necessary for most applications. Nano-scale, deformation twinned copper microstructures exhibit a rare combination of strength and stability. While storing less energy in their interfaces than other nanostructured metals, they also exhibit lower vacancy supersaturations, reducing the driving force and mobility for microstructure evolution. From a thermal stability perspective, the nano-twinned microstructure may thus be preferred over the more commonly produced nano-scale equiaxed microstructures.

Keywords

copper, crystal microstructure, deformation, nanostructured materials, thermal stability, twinning, vacancies (crystal)

Disciplines

Materials Science and Engineering

Comments

This article appeared in *Applied Physics Letters*, 99, no. 23 (2011): 231911 and may be found at <http://dx.doi.org/10.1063/1.3669404>.

Rights

Copyright 2011 American Institute of Physics. This article may be downloaded for personal use only. Any other use requires prior permission of the author and the American Institute of Physics.

Vacancies, twins, and the thermal stability of ultrafine-grained copper

C. Saldana, A. H. King, E. A. Stach, W. D. Compton, and S. Chandrasekar

Citation: *Appl. Phys. Lett.* **99**, 231911 (2011); doi: 10.1063/1.3669404

View online: <http://dx.doi.org/10.1063/1.3669404>

View Table of Contents: <http://apl.aip.org/resource/1/APPLAB/v99/i23>

Published by the [American Institute of Physics](#).

Related Articles

Dopant mapping of Be δ -doped layers in GaAs tailored by counterdoping using scanning tunneling microscopy
Appl. Phys. Lett. **101**, 192103 (2012)

Indicators of mobility extraction error in bottom gate CdS metal-oxide-semiconductor field-effect transistors
Appl. Phys. Lett. **101**, 182106 (2012)

Fermi-level unpinning and low resistivity in contacts to n-type Ge with a thin ZnO interfacial layer
Appl. Phys. Lett. **101**, 182105 (2012)

Structural incommensurate modulation rule in hexagonal Ba(Ti_{1-x}M_x)O_{3- δ} (M = Mn, Fe) multiferroics
AIP Advances **2**, 042129 (2012)

Electron paramagnetic resonance and theoretical studies of Nb in 4H- and 6H-SiC
J. Appl. Phys. **112**, 083711 (2012)

Additional information on *Appl. Phys. Lett.*

Journal Homepage: <http://apl.aip.org/>

Journal Information: http://apl.aip.org/about/about_the_journal

Top downloads: http://apl.aip.org/features/most_downloaded

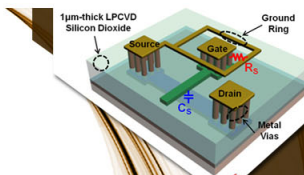
Information for Authors: <http://apl.aip.org/authors>

ADVERTISEMENT



**EXPLORE WHAT'S
NEW IN APL**

SUBMIT YOUR PAPER NOW!



SURFACES AND INTERFACES

Focusing on physical, chemical, biological, structural, optical, magnetic and electrical properties of surfaces and interfaces, and more...



ENERGY CONVERSION AND STORAGE

Focusing on all aspects of static and dynamic energy conversion, energy storage, photovoltaics, solar fuels, batteries, capacitors, thermoelectrics, and more...

Vacancies, twins, and the thermal stability of ultrafine-grained copper

C. Saldana,¹ A. H. King,^{2,a)} E. A. Stach,³ W. D. Compton,⁴ and S. Chandrasekar⁴

¹*Harold and Inge Marcus Department of Industrial and Manufacturing Engineering, The Pennsylvania State University, University Park, Pennsylvania 16802, USA*

²*The Ames Laboratory, Ames, Iowa 50011-3020, USA*

³*Center for Functional Nanomaterials, Brookhaven National Laboratory, Upton, New York 11973-5000, USA*

⁴*Center for Materials Processing and Tribology, School of Industrial Engineering, Purdue University, West Lafayette, Indiana 47907-2023, USA*

(Received 22 September 2011; accepted 18 November 2011; published online 9 December 2011)

Ultrafine-grained metals have impressive strength but lack the thermal stability necessary for most applications. Nano-scale, deformation twinned copper microstructures exhibit a rare combination of strength and stability. While storing less energy in their interfaces than other nanostructured metals, they also exhibit lower vacancy supersaturations, reducing the driving force and mobility for microstructure evolution. From a thermal stability perspective, the nano-twinned microstructure may thus be preferred over the more commonly produced nano-scale equiaxed microstructures.

© 2011 American Institute of Physics. [doi:10.1063/1.3669404]

Conventional microstructure stabilization methods for ultrafine-grained (UFG) metals are limited by their incompatibility with high-purity single-phase systems. For these metals, control of the final defect structure, the particular configuration of grain boundaries, and triple junctions and quadruple points are the primary means of influencing thermal stability. Here we demonstrate UFG microstructure stabilization in copper through a high density of twin boundaries. A dense nano-scale network of twins can be introduced using high-rate, pulsed deposition^{1–3} or severe plastic deformation (SPD).^{4–6} Interest in nano-twinned microstructures stems from the finding that twin interfaces support pile-ups and yet provide for dislocation accommodation, thereby enhancing strength and ductility simultaneously.^{2,7} Twinned microstructures also have demonstrated enhanced electrical performance, fracture toughness, and stability against cyclic loading.^{3,8–10} Encouraging observations of stability against thermal exposure relative to conventional UFG microstructures have been made for nano-scale copper growth twins^{1,11} but were based on measurements scattered across multiple studies, leaving uncertainty regarding variance arising from differences in experimental method. Enhanced thermal stability has yet to be reported for microstructures with nano-scale deformation twins. We show here that, at comparable strength, such microstructures are thermally more stable than conventional SPD microstructures (equiaxed and UFG) due to the combination of a reduced driving force and a lower mobility for microstructure evolution associated with reduced vacancy supersaturation. This finding has implications for the application of UFG materials in radiation environments.

Oxygen-free high conductivity copper (99.99% purity) with a grain size of $415\ \mu\text{m} \pm 40\ \mu\text{m}$ and hardness of $72 \pm 5\ \text{kg}/\text{mm}^2$ was subjected to shear strains of $\gamma \sim 1, 2,$ and 4 by machining at near ambient and cryogenic temperatures. The strain rate under these conditions was determined to be $\sim 10^3/\text{s}$, based on image correlation measurements.⁵ Thermal

stability was assessed using microindentation and differential scanning calorimetry (DSC). The DSC was carried out under heating rates of $\beta = 10, 20,$ and $30\ \text{K}/\text{min}$ to facilitate estimation of activation energy. The difference in peak recrystallization temperature between heating rates was $5\text{--}10\ \text{K}$. Activation energy was determined following Kissinger's analysis, where the slope of a linear fit of $\ln(\beta/T_p^2)$ versus $1/T_p$ yields Q/R , where T_p is the peak temperature and R the gas constant. Transmission electron microscopy (TEM) samples were prepared by electrolytic thinning; these were observed with a FEI Tecnai TEM at 200 kV. Grain size and twin spacing measurements were made following Heyn's line intercept method and twin volume fraction from the procedure outlined in Ref. 12.

Figure 1(a) shows the evolution of hardness with increasing strain. The greater hardness of the cryogenically deformed samples is expected, due to the suppressed annihilation of dislocations by retardation of dislocation climb and cross slip at low temperature. Figure 1(a) also shows that the strain and deformation temperature influenced recrystallization kinetics. For samples deformed at ambient, recrystallization occurred at temperatures dropping from 510 to 425 K with increasing strain. Recrystallization occurred from 485 to 375 K for corresponding samples deformed cryogenically. The increase of strength and reduction of stability with increasing strain and decreasing deformation temperature are further evident in Fig. 1(b), where a negative correlation between recrystallization temperature and hardness is evident. Fig. 1(b) shows that copper deformed at $\gamma \sim 4$ at ambient temperature (point A4) had a hardness of $\sim 155\ \text{kg}/\text{mm}^2$ and a recrystallization temperature of $\sim 425\ \text{K}$. This is consistent with characteristic hardness saturation and thermal stability of UFG copper.⁵ While the negative correlation holds for most data points (ambient and cryogenic), an efficient combination of strength and stability is apparent in samples deformed cryogenically at $\gamma \sim 1$ (point C1). This condition gave a hardness of $\sim 155\ \text{kg}/\text{mm}^2$ and a recrystallization temperature of $\sim 485\ \text{K}$, a thermal stability $\sim 60\ \text{K}$ higher than that suggested by the trend.

^{a)}Author to whom correspondence should be addressed. Electronic mail: alexking@ameslab.gov. Tel.: +1 515-294-2770.

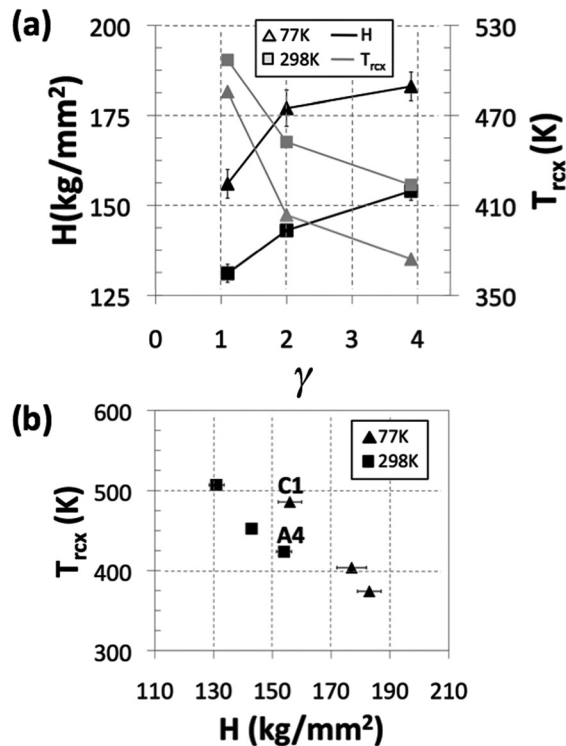


FIG. 1. Effect of shear strain (γ) on hardness (H) and recrystallization temperature (T_{recx}). (b) T_{recx} as a function of H . Standard deviation for temperature was small (<3 K). Points A4 and C1 correspond to copper deformed at (298 K, $\gamma \sim 4$) and (77 K, $\gamma \sim 1$), respectively.

Contributions to hardening for metals can come from multiple sources, including point-defects, dislocation intersections, grain boundaries, and twin boundaries in differing amounts. Thus, it is unsurprising that the correlation between hardening and thermal instability cannot be explained across all cases using a simple linear relationship, so we seek unifying principles from thermodynamic measurements. The total energy released during recrystallization provides the driving force for this transformation, and it ranged from 35 to 85 J/mol for the samples deformed at ambient and from 55 to 165 J/mol for samples deformed cryogenically [Fig. 2(a)]. Figure 2(b) shows the relationship between thermal stability and stored energy in the present work and other studies.^{13–15} Recrystallization temperature follows a power law dependence on stored energy and the annealing response of the low strain cryogenic sample, which fell apart from the trend in Fig. 1(b), lies on the trendline in Fig. 2(b).

The microstructures developed at $\gamma \sim 4$ (ambient) and $\gamma \sim 1$ (cryogenic), shown in Fig. 3(a), are of interest due to their similar strength but different thermal stability. The microstructure developed at $\gamma \sim 4$ (ambient) is typical of conventional SPD—uniform and equiaxed with a grain size of 207 ± 26 nm (Inset A4).⁵ The microstructure evolved at $\gamma \sim 1$ (cryogenic) was substantially different and more heterogeneous, with pre-existing grains consisting almost entirely either of deformation twins (insets C1-I and C1-II) or the more usual dislocation arrangements, e.g., cells (inset C1-III). The importance of twinning-mediated plasticity at low deformation temperature is well known for metals with moderate stacking fault energy, such as copper. The heterogeneity in these microstructures might be expected due to the dependence of twinning probab-

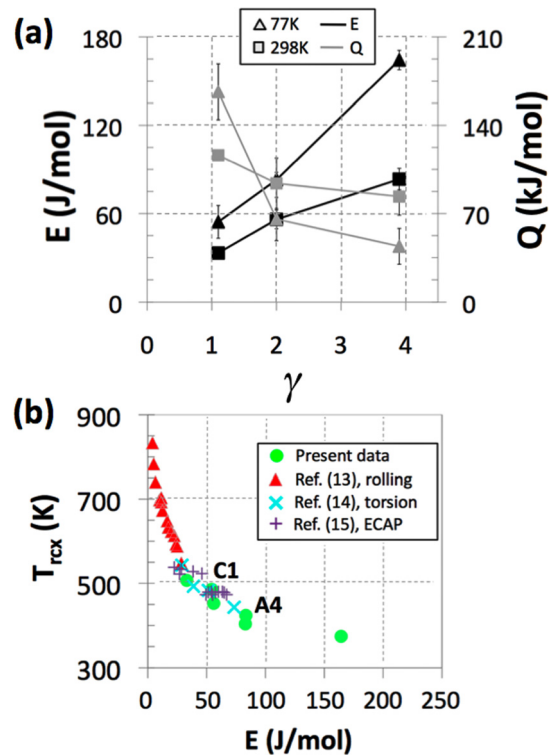


FIG. 2. (Color online) (a) Effect of shear strain (γ) on stored energy (E) and activation energy (Q). (b) Recrystallization temperature (T_{recx}) as a function of E . Points A4 and C1 correspond to copper deformed at (298 K, $\gamma \sim 4$) and (77 K, $\gamma \sim 1$), respectively.

ity on the orientation of the shear direction with respect to the crystal. For this condition, the twin volume fraction (V_{twin}) was 0.4 and the twin spacing was $d_{\text{twin}}(\mu, \sigma) \sim (50 \text{ nm}, 36 \text{ nm})$. Individual measurements of d_{twin} are summarized in Fig. 3(b) and generally followed a lognormal distribution.

These microstructure observations and calorimetric measurements correlate the presence of dense nano-twin boundaries with enhanced thermal stability. Observations of thermal stability in nano-scale growth twins have elsewhere been attributed to the low free energy of the coherent twin, which is a fraction (~ 0.03) of that of a general high angle grain boundary (HAGB).^{1,11} While this reasoning might be

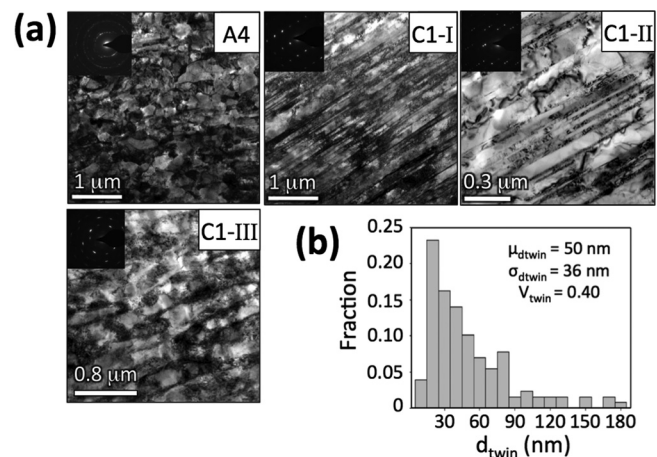


FIG. 3. (a) Representative micrographs of copper deformed at 298 K and $\gamma \sim 4$ (inset A4), 77 K and $\gamma \sim 1$ (insets C1-I to C1-III). (b) Histogram of twin spacing for copper deformed at 77 K and $\gamma \sim 1$.

applied in the present study, the structures of deformation twins can vary from those of growth twins due to interactions with defects that alter the interface and elevate free energy. In this regard, twin boundary energy likely increases with strain, as increased deformation levels promote the generation of a greater number of defects. Indeed, the free energy of deformation twins created elsewhere at higher strain ($\gamma \sim 3.8$), and cryogenic temperature was observed to approach that of general HAGBs.¹⁶ The twin interfaces in the present study were produced at a lower strain ($\gamma \sim 1$); this would yield smaller final defect densities.

The enhanced stability of twinned structures can be also impacted by deformation-induced vacancies. Vacancy supersaturations enhance kinetics by aiding nucleation and enhancing grain boundary mobility.¹⁷ They can also provide a driving force for grain growth, as migrating boundaries leave relatively defect-free, lower-energy material in their wake. The concentration of vacancies in deformed copper can exceed 10^{-4} ,¹⁸ and vacancy content is expected to be higher after large strain and low temperature deformation due to high vacancy production and reduced kinetics of vacancy migration to sinks, respectively.

The kinetics of any vacancy-mediated process, such as self-diffusion, usually depend upon the probability of a vacancy being present and the probability of the vacancy crossing the energy barrier for the process to occur. Because these probabilities are multiplied, the measured activation energy is the sum of the vacancy formation energy, Q_{vf} , and the activation energy for vacancy migration, Q_{vm} , if the process occurs in an equilibrium vacancy concentration. The probability of a process occurring in unit time is given by

$$\text{Rate} \propto P_{eq} = X_1 e^{-Q_{vf}/RT} X_2 e^{-Q_{vm}/RT} = X_1 X_2 e^{-(Q_{vf}+Q_{vm})/RT},$$

where X_1 and X_2 are constants, R is the gas constant, and T is the absolute temperature. If there is a vacancy supersaturation, then the probability of a vacancy being present is increased, and the rate equation for the supersaturated case becomes

$$\begin{aligned} \text{Rate} \propto P_{ss} &= (S + X_1 e^{-Q_{vf}/RT}) X_2 e^{-Q_{vm}/RT} \\ &= S X_2 e^{-Q_{vm}/RT} + X_1 X_2 e^{-(Q_{vf}+Q_{vm})/RT}, \end{aligned}$$

where S is the mole fraction of vacancies above the equilibrium level. In this case the apparent activation energy is a weighted mean of Q_{vm} and $(Q_{vf} + Q_{vm})$, more closely approaching Q_{vm} as the supersaturation increases.

These effects are clear in the measured activation energies for recrystallization. Figure 2(a) shows the activation energies for the samples deformed at ambient temperature. These all lie between the activation energy for vacancy migration ($Q_{vm} \sim 71$ kJ/mol) and that for self-diffusion in copper ($Q_{sd} \sim 196$ kJ/mol). The activation energy for self diffusion is (within experimental error) the sum of the vacancy formation energy ($Q_{vf} \sim 123$ kJ/mol) and the migration energy. For the samples deformed at higher strain and at cryogenic temperature, the activation energy fell in the range of 45–65 kJ/mol, corresponding to significantly raised vacancy concentrations. For the densely twinned samples, the

activation energy was markedly larger, approaching 165 kJ/mol, implying that a smaller vacancy supersaturation affects the recrystallization kinetics for these microstructures. This would occur if twin boundaries are efficient sinks for vacancies produced during deformation, or if the deformation process leading to the twinned microstructure does not produce vacancies at the same rate as the processes leading to dislocation cell walls. Although twins may be efficient point-defect sinks,¹⁹ their operation during low temperature deformation is questionable because of suppression of thermally activated vacancy migration. Furthermore, vacancy production during deformation is generally associated with the intersection of extended dislocations, forming complex jogs that act as vacancy sources. This process would be expected to be absent if deformation occurs by twinning.

The thermal instability of conventional UFG copper has been linked to excess vacancy concentrations:²⁰ our results corroborate this finding and demonstrate that reducing vacancy supersaturation can improve stability. Nano-twinned materials produced by growth methods likely contain vacancy supersaturations that differ from our SPD specimens and may therefore behave somewhat differently. Direct measurements of vacancy content in twinned samples will help establish details of the stabilization mechanism. Vacancy content clearly degrades stability, and its minimization is an important aspect of process design for nano-scaled materials. In view of this, these materials should be used in radiation environments only with the greatest caution.

This work was supported by NSF CMMI grants 1130852 (Penn State) and 0928337/0800481 (Purdue), US-DOE contracts DE-AC02-98CH10886 (Brookhaven National Laboratory), and DE-AC02-07CH11358 (Ames Laboratory).

¹O. Anderoglu, A. Misra, H. Wang, and X. Zhang, *J. Appl. Phys.* **103**, 094322 (2008).

²K. Lu, L. Lu, and S. Suresh, *Science* **324**, 349 (2009).

³L. Lu, Y. F. Shen, X. H. Chen, L. H. Qian, and K. Lu, *Science* **304**, 422 (2004).

⁴C. Saldana, T. G. Murthy, M. R. Shankar, E. A. Stach, and S. Chandrasekar, *Appl. Phys. Lett.* **94**, 021910 (2009).

⁵T. L. Brown, C. Saldana, T. G. Murthy, J. B. Mann, Y. Guo, L. F. Allard, A. H. King, W. D. Compton, K. P. Trumble, and S. Chandrasekar, *Acta Mater.* **57**, 5491 (2009).

⁶Y. S. Li, Y. Zhang, N. R. Tao, and K. Lu, *Acta Mater.* **57**, 761 (2009).

⁷Y. Wang, M. Chen, F. Zhou, and E. Ma, *Nature* **419**, 912 (2002).

⁸K. C. Chen, W. Wu, C. Liao, L. Chen, and K. Tu, *Science* **321**, 1066 (2008).

⁹C. J. Shute, B. D. Myers, S. Xie, T. W. Barbee, A. M. Hodge, and J. R. Weertman, *Scr. Mater.* **60**, 1073 (2009).

¹⁰E. W. Qin, L. Lu, N. R. Tao, and K. Lu, *Scr. Mater.* **60**, 539 (2009).

¹¹X. Zhang, O. Anderoglu, R. G. Hoagland, and A. Misra, *JOM* **60**, 75 (2008).

¹²E. E. Underwood and W. C. Coons, in *Deformation Twinning*, edited by R. E. Reed-Hill, J. P. Hirth, and H. C. Rodgers (Gordon & Breach, New York, 1964), p. 405.

¹³D. Mandal and I. Baker, *Scr. Metall. Mater.* **33**, 645 (1995).

¹⁴L. M. Clarebrough, M. E. Hargreaves, D. Michell, and G. W. West, *Proc. R. Soc. A* **215**, 507 (1952).

¹⁵Y. Zhang, J. T. Wang, C. Cheng, and J. Liu, *J. Mater. Sci.* **43**, 7326 (2008).

¹⁶H. L. Wang, Z. B. Wang, and K. Lu, *Acta Mater.* **59**, 1818 (2011).

¹⁷M. Feller-Kniepmeier and J. Gorbrecht, *Acta Metall.* **19**, 569 (1971).

¹⁸T. Ungar, E. Schafner, P. Hanak, S. Bernstorff, and M. J. Zehetbauer, *Mater. Sci. Eng. A* **462**, 398 (2007).

¹⁹A. H. King and D. A. Smith, *Philos. Mag. A* **42**, 495 (1980).

²⁰W. Q. Cao, C. F. Gu, E. V. Pereloma, and C. H. J. Davies, *Mater. Sci. Eng. A* **492**, 74 (2008).